# Hexagonal Sampling

*Marta Woodward* and *Francis Muir*

## Introduction

Two-dimensional geophysical surveys are traditionally implemented on rectangular sampling lattices. While it has been known for some time that circularly bandlimited signals are sampled 13.4% more efficiently by hexagonal lattices than by rectangular lattices (Peterson and Middleton, 1962), only recently has it been shown that processing algorithms for hexagonal systems are similarly 25-50% more efficient than those for rectangular systems with the same frequency resolution (Mersereau, 1979). As potential or seismic wave fields in areas of unknown structure are most reasonably assumed circularly bandlimited in map view, adoption of these new hexagonal sampling strategies could theoretically increase the efficiency of current two-dimensional surveys by 13-50%. These ideas are particularly interesting for 3-d seismic applications, where present processing costs are often prohibitively high. Following is a summary of hexagonal sampling theory and processing algorithms, drawn from the references listed at the end of the paper.

## Two-Dimensional Sampling Theory

Periodic sampling in one dimension may be described as multiplication by a comb function

$$\hat{f}(t) = \sum_{k=-\infty}^{\infty} f(kT)\delta(t - kT), \tag{1}$$

where T is the sampling interval. In the wave-number domain this corresponds to convolution with another comb function

$$\tilde{F}(\omega) = F(\omega) * \frac{2\pi}{T} \sum_{k=-\infty}^{\infty} \delta(\omega - \frac{2\pi k}{T}) = \frac{2\pi}{T} \sum_{k=-\infty}^{\infty} F(\omega + \frac{2\pi k}{T}) \tag{2}$$

and consequently replication along the $\omega$ axis. Sampling theory shows that $f(t)$ may be exactly interpolated from $\hat{f}(t)$ when $F(\omega)$ is recoverable from $\tilde{F}(\omega)$ through windowing—*i.e.* when $F(\omega)$ is replicated without overlapping. For a bandlimited $f(t)$ ($F(\omega) = 0$ for $|\omega| \geq \frac{R}{2}$), this requirement is met when $T \leq \frac{2\pi}{R}$. Sampling efficiency is always maximized by choosing $T = \frac{2\pi}{R}$.

Periodic sampling in two dimensions may similarly be described as multiplication by an impulse field in the time domain and convolution (replication) with the transformed impulse field in the wave-number domain. For a rectangular sampling lattice these operations produce

$$\hat{f}(t_1, t_2) = \sum_{k_1} \sum_{k_2} f(k_1 T_1, k_2 T_2) \delta(t_1 - k_1 T_1) \delta(t_2 - k_2 T_2) \tag{3}$$

$$\begin{aligned} \tilde{F}(\omega_1, \omega_2) &= F(\omega_1, \omega_2) * \frac{4\pi^2}{T_1 T_2} \delta(\omega_1 - k_1 \frac{2\pi}{T_1}) \delta(\omega_2 - k_2 \frac{2\pi}{T_2}) \\ &= \sum_{k_1} \sum_{k_2} \frac{4\pi^2}{T_1 T_2} F(\omega_1 + k_1 \frac{2\pi}{T_1}, \omega_2 + k_2 \frac{2\pi}{T_2}) \end{aligned} \tag{4}$$

where $T_1$ and $T_2$ are the sampling intervals defined in Figure 1. Since a hexagonal lattice may always be formed through superposition of two offset rectangular lattices, generalized hexagonal sampling equations are

$$\begin{aligned} \hat{f}(t_1, t_2) &= f(t_1, t_2) \sum_{k_1} \sum_{k_2} \Big[ \delta(t_1 - k_1 T_1) \delta(t_2 - 2k_2 T_2) \\ &\qquad + \delta(t_1 - (k_1 + \frac{1}{2}) T_1) \delta(t_2 - (2k_2 + 1) T_2) \Big] \\ &= f(\frac{2k_1 - k_2}{2} T_1, k_2 T_2) \sum_{k_1} \sum_{k_2} \delta(t_1 - \frac{2k_1 - k_2}{2} T_1) \delta(t_2 - k_2 T_2) \end{aligned} \tag{5}$$

$$\begin{aligned} \tilde{F}(\omega_1, \omega_2) &= F(\omega_1, \omega_2) * \frac{2\pi^2}{T_1 T_2} \sum_{k_1} \sum_{k_2} \delta(\omega_1 - k_1 \frac{2\pi}{T_1}) \delta(\omega_2 - k_2 \frac{\pi}{T_2}) (1 + (-1)^{k_1 + k_2}) \\ &= \frac{4\pi^2}{T_1 T_2} \sum_{k_1} \sum_{k_2} F(\omega_1 + (2k_1 - k_2) \frac{2\pi}{T_1}, \omega_2 + k_2 \frac{\pi}{T_2}). \end{aligned} \tag{6}$$

Note that rectangular and hexagonal sampling lattices transform into rectangular and hexagonal replication (aliasing) lattices, respectively.

The rectangular and hexagonal sampling processes are pictured in Figure 1 as tilings of the Fourier plane with interlocking tiles of fixed area $\frac{4\pi^2}{T_1 T_2}$. As in the one-dimensional case, interpolation of a bandlimited $f(t_1, t_2)$ ($F(\omega_1, \omega_2) = 0$ for $(\omega_1, \omega_2) \notin R$) from $\hat{f}(t_1, t_2)$ is

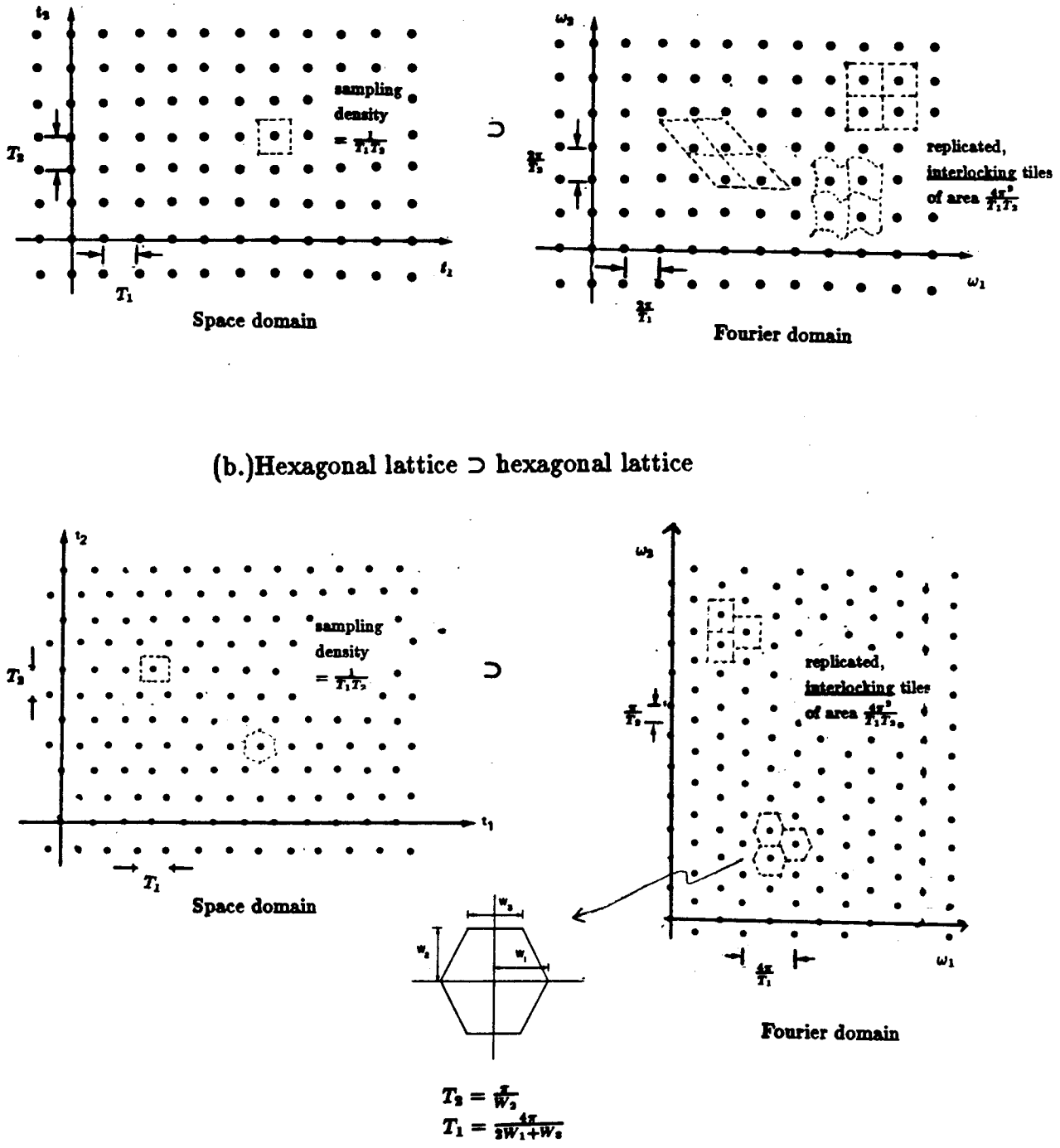


FIG. 1. Two dimensional sampling.

possible when $F(\omega_1, \omega_2)$ is replicated without overlapping—*i.e.* when $R$ may be inscribed within one of the replicated tiles. Since impulse intervals in the space and Fourier domains are inversely related, sampling density is proportional to the area of the replicated tile shape and sampling efficiency is maximized when replicated $F(\omega_1, \omega_2)$'s are packed together as closely as possible. This relation implies circularly bandlimited functions ($F(\omega_1, \omega_2) = 0$ for $\omega_1^2 + \omega_2^2 > \Omega^2$) may be sampled **13.4%** more efficiently by a regular, hexagonal lattice than by a square lattice (see Figure 2). Furthermore, from body-centered-cubic type arguments, it is clear that hexagonal sampling is the most efficient sampling pattern possible (given that the Fourier plane can't be tiled with polygons of more than six sides).

## Processing Hexagonal Sequences

This saving in sampling density for circularly bandlimited functions is augmented when the hexagonal sequences are processed. Following are derivations of Fourier transform, DFT and FFT equations for hexagonally sampled sequences. Because hexagonal sampling is primarily important for circularly bandlimited functions, the arguments will be limited to a space domain sampling lattice with $T_1 = \frac{2}{\sqrt{3}}$ and $T_2 = 1$—corresponding to regular ($W_1 = W_3 = \frac{2W_2}{\sqrt{3}}$), normalized ($W_2 = \pi$) hexagonal tiles in the wavenumber domain (Figure 1). A lattice of this design will recover a circular bandregion of radius $\pi$ with maximum efficiency (Figure 2).

### A. Fourier Transforms

Substituting these values for $T_1$ and $T_2$ into equation (5) and Fourier transforming the hexagonally sampled sequence yields

$$\begin{aligned}\tilde{F}(\omega_1,\omega_2) &= \int_{-\infty}^{\infty}\int_{-\infty}^{\infty}\sum_{k_1}\sum_{k_2} f\left(\frac{2k_1-k_2}{\sqrt{3}},k_2\right)\delta\left(t_1-\frac{2k_1-k_1}{\sqrt{3}}\right)\delta(t_2-k_2) \\ &\qquad \cdot exp(-i\omega_1 t_1 - i\omega_2 t_2)dt_1 dt_2 \\ &= \sum_{k_1}\sum_{k_2} f\left(\frac{2k_1-k_2}{\sqrt{3}},k_2\right) exp\left[-i\left(\frac{2k_1-k_2}{\sqrt{3}}\omega_1 + k_2\omega_2\right)\right] \\ &= \sum_{k_1}\sum_{k_2} f'(k_1,k_2) exp\left[-i\left(\frac{2k_1-k_2}{\sqrt{3}}\omega_1 + k_2\omega_2\right)\right] \qquad (7)\end{aligned}$$

where the sudden appearance of $f'(k_1, k_2)$ results from introduction of the primed (affine) coordinate system of Figure 3. Inverse Fourier transforming over one period ($R$) of

**Case I.:** Circularly bandlimited function ($F(\omega_1, \omega_2) = 0$ for $\omega_1^2 + \omega_2^2$) sampled without aliasing by a square lattice ($T_1 = \frac{\pi}{W}, T_2 = \frac{\pi}{W}$) of sampling density $\frac{W^2}{\pi^2}$

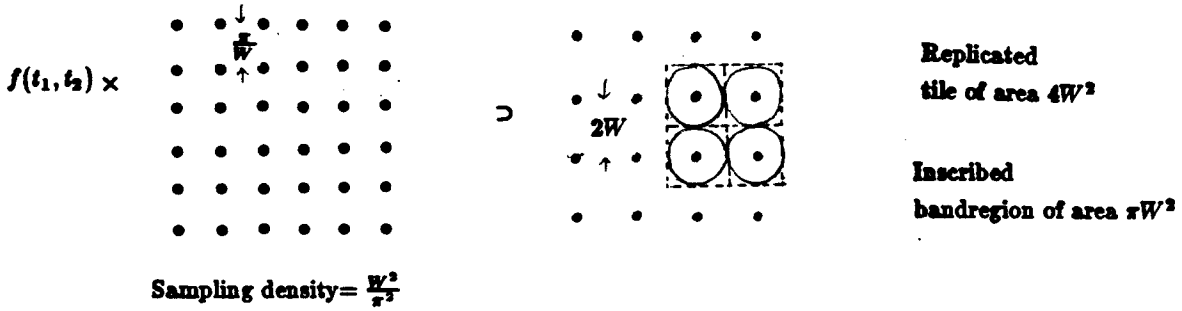


Sampling density= $\frac{W^2}{\pi^2}$

**Case II.:** Circularly bandlimited function ($F(\omega_1, \omega_2) = 0$ for $\omega_1^2 + \omega_2^2 > \omega^2$) sampled without aliasing by a hexagonal lattice ($T_1 = \frac{2\pi}{\sqrt{3}W}, T_2 = \frac{\pi}{W}$) of sampling density $\frac{\sqrt{3}\omega^2}{2\pi^2}$.

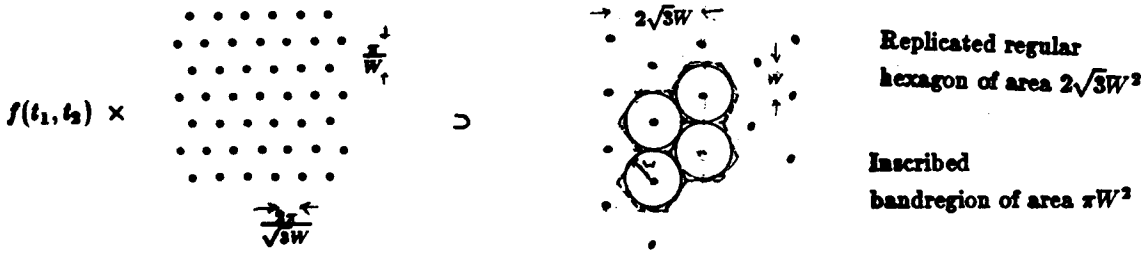


Sampling density= $\frac{\sqrt{3}W^2}{2\pi^2}$

**Conclusion:**

$$\frac{\text{Sampling density of nonaliasing hexagonal lattice}}{\text{Sampling density of nonaliasing square lattice}} = \frac{\sqrt{3}}{2}$$

**A hexagonal sampling lattice of $\frac{T_1}{T_2} = \frac{2}{\sqrt{3}}$ (which produces a regular hexagonal replication lattice) is 13.4% more efficient at sampling a circularly bandlimited function than a square lattice ($\frac{T_1}{T_2} = 1$).**

FIG. 2. Hexagonal vs. rectangular sampling efficiency for circularly bandlimited signals.

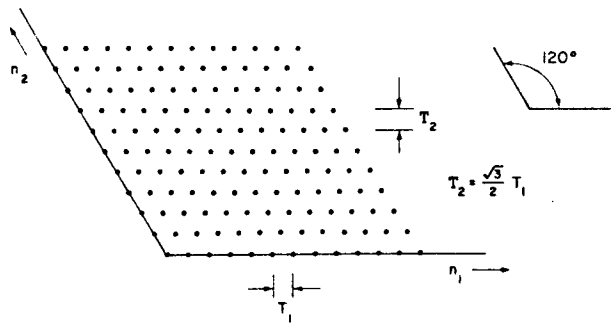


FIG. 3. Hexagonal coordinate system (Gallagher and Murphy, 1982).

$\tilde{F}(\omega_1, \omega_2)$ to recover $f'(k_1, k_2)$ produces

$$f'(k_1,k_2) = \frac{1}{2\pi^2\sqrt{3}} \int_R \int \tilde{F}(\omega_1,\omega_2) exp\left[i\left(\frac{2k_1 - k_2}{\sqrt{3}}\omega_1 + k_2\omega_2\right)\right] d\omega_1 d\omega_2. \quad (8)$$

The difficult integration over hexagon $R$ may be avoided by integrating instead over a square containing 2 periods and halving the result

$$f'(k_1,k_2) = \frac{1}{4\pi^2\sqrt{3}} \int_{-\pi}^{\pi} \int_{-\pi\sqrt{3}}^{\pi\sqrt{3}} \tilde{F}(\omega_1,\omega_2) exp\left[i\left(\frac{2k_1 - k_2}{\sqrt{3}}\omega_1 + k_2\omega_2\right)\right] d\omega_1 d\omega_2. \quad (9)$$

Equations (7) and (9) are the forward and inverse Fourier transform equations for sequences $f'(k_1, k_2)$, collected on hexagonal lattices with $T_1 = \frac{2}{\sqrt{3}}$ and $T_2 = 1$. They may be used to prove that: (1) rectangular Fourier transform properties (linearity, shift, convolution, Parseval's relation, etc.) hold for hexagonal systems, and (2) hexagonally sampled complex sinusoids ($exp\left[-i\left(\frac{2k_1-k_2}{\sqrt{3}}\omega_1 + k_2\omega_2\right)\right]$) are the eigensequences of hexagonal linear shift-invariant systems.

B. Discrete Fourier transforms

The DFT of a sequence of numbers is the Fourier transform of a replicated version of that sequence, evaluated over one period in the wave-number domain; equivalently, it is a sampling of the sequence's periodic Fourier transform over one period. These operations correspond to Fourier transforming after convolving with a periodic impulse field in the space domain and multiplying by a periodic impulse field in the wave-number domain, respectively. Consequently, for the sampling and replication lattices illustrated in Figure 4, the DFT is defined by

$$\tilde{F}(k_1,k_2) = \tilde{F}(\omega_1,\omega_2) \sum_{k_1} \sum_{k_2} \delta\left(\omega_1 - \frac{2k_1 - k_2}{2} \frac{4\pi}{(2M_1 + M_2)T_1}\right) \delta\left(\omega_2 - k_2 \frac{\pi}{M_2 T_2}\right). \quad (10)$$

Hexagonal periodicity: $\tilde{f}(n_1, n_2) = \tilde{f}(n_1 - M_1 - M_2, n_2 - M_2)$

$= \tilde{f}(n_1 - 2M_1 - M_2, n_2)$

$= \tilde{f}(n_1 - M_2, n_2 - 2M_2)$

for regular hexagons
$M_1 = M_2 = M$

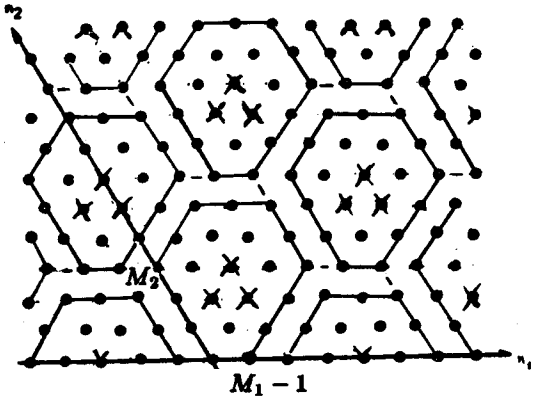


Fundamental period as hexagon

$R_H(M_1, M_2)$ =one period
$= (2M_1 + M_2)M_2$ points

$M_1 = 2 \quad M_2 = 3$

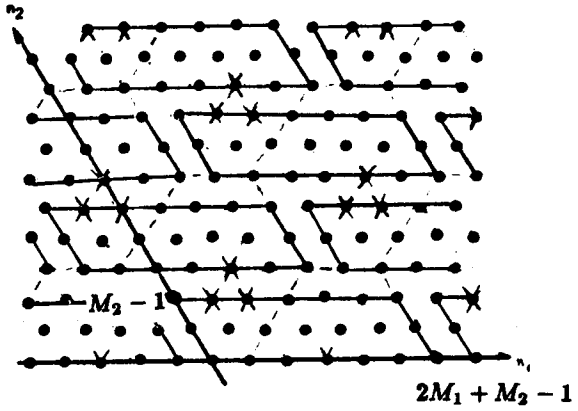


Fundamental period as parallelogram

$R_p(M_1, M_2)$ =one period
$= (2M_1 + M_2)M_2$ points
(more obviously)

FIG. 4. Hexagonal periodicity.

Reintroducing the skewed axes of Figure 3, dropping the primes, using equation (7), and setting ($T_1 = \frac{2}{\sqrt{3}}, T_2 = 1$) yields

$$\tilde{F}(k_1,k_2) = \tilde{F}\left(\frac{2k_1-k_2}{2M_1+M_2}\pi\sqrt{3}, k_2\frac{\pi}{M_2}\right)$$
$$= \sum_{n_1=0}^{2M_1+M_2-1}\sum_{n_2=0}^{M_2-1} f(n_1,n_2)exp\left(-i\left[\frac{(2n_1-n_2)(2k_1-k_2)}{2M_1+M_2}\pi + n_2k_2\frac{\pi}{M_2}\right]\right)$$

$$(n_1,n_2),\ (k_1,k_2) \in R_P(M_1,M_2). \tag{11}$$

The sums over $n_1$ and $n_2$ are taken over the fundamental period of $\tilde{f}(n_1,n_2)$ in its parallelogram rather than hexagon form for the purpose of simplifying the computation (Figure 4). Using similar reasoning, the inverse DFT may be described as

$$\tilde{f}(n_1,n_2) = \frac{1}{(2M_1+M_2)M_2}\sum_{k_1=0}^{2M_2+M_1-1}\sum_{k_2=0}^{M_2-1}\tilde{F}(k_1,k_2)$$
$$\cdot \exp\left(i\left[\frac{(2n_1-n_2)(2k_1-k_2)}{(2M_1+M_2)}\pi + n_2k_2\frac{\pi}{M_2}\right]\right)$$

$$(k_1,k_2),\ (n_1,n_2) \in R_P(M_1,M_2). \tag{12}$$

For arguments identical to those presented in the section on two-dimensional sampling, it can be shown the frequency resolution (sampling density in the Fourier domain) associated with any DFT is maximized when the replication lattice is regular hexagonal—when $M_1 = M_2 = M$. For this case a regular hexagonal DFT requires 25% fewer samples than a square DFT with comparable resolution ($3M^2$ versus $4M^2$ samples) and the DFT equations become

$$\tilde{F}(k_1,k_2) = \sum_{n_1=0}^{3M-1}\sum_{n_2=0}^{M-1} f(n_1,n_2)exp\left(-i\left[(2n_1-n_2)(2k_1-k_2)\frac{\pi}{3M} + n_2k_2\frac{\pi}{M}\right]\right)$$

$$(n_1,n_2),\ (k_1,k_2) \in R_P(M,M). \tag{13}$$

$$\tilde{f}(n_1,n_2) = \frac{1}{3M^2}\sum_{k_1=0}^{3M-1}\sum_{k_2=0}^{M-1}\tilde{F}(k_1,k_2)exp\left(i\left[(2n_1-n_2)(2k_1-k_2)\frac{\pi}{3M} + n_2k_2\frac{\pi}{M}\right]\right)$$

$$(k_1,k_2),\ (n_1,n_2) \in R_P(M,M). \tag{14}$$

Figure 5 shows single bandregion DFT pairs for three hexagonally sampled functions: an impulse/plane, an infinite vertical impulse sheet/infinite horizontal impulse sheet, and a truncated vertical impulse sheet/modulated (sinc-like) infinite horizontal impulse sheet. While the pairs are related as expected, the last two are modified by unusual wraparound behavior. Because neighboring hexagonal tiles (replicating bandregions) are offset from each other in the horizontal direction, an infinite horizontal sheet will always wrap through a hexagon twice, symmetrically around the long axis. The same phenomenon occurs for vertical features cutting through the corner regions.

C.Fast Fourier transforms

The kernel for the hexagonal DFT is inseparable. While this condition prevents application of two successive one-dimensional FFT's, it does not interfere with implementation of Rivard's faster, vector radix algorithm (a Cooley-Tukey type decimation in 2 dimensions). Requiring M to be a power of two, the $DFT_M[f(n_1,n_2)]$—$\tilde{F}(k_1,k_2)$—may be broken down into four separate sums for the cases $k_1/k_2$: even/even, even/odd, odd/even and odd/odd—

$$\begin{aligned}\tilde{F}(k_1,k_2) = {} & DFT_{\frac{M}{2}}[f(2r_1,2r_2)] \\ & + exp\left[i\frac{2\pi}{3M}(k_1-2k_2)\right]\cdot DFT_{\frac{M}{2}}[f(2r_1,2r_2+1)] \\ & + exp\left[-i\frac{2\pi}{3M}(2k_1-k_2)\right]\cdot DFT_{\frac{M}{2}}[f(2r_1+1,2r_2)] \\ & + exp\left[-i\frac{2\pi}{3M}(k_1+k_2)\right]\cdot DFT_{\frac{M}{2}}[f(2r_1+1,2r_2+1)]. \end{aligned} \tag{15}$$

Just as $\tilde{F}(k_1,k_2)$ is hexagonally periodic with period M, each of the $DFT_{\frac{M}{2}}$'s is hexagonally periodic with period $\frac{M}{2}$. Consequently, the DFT may be represented by

$$\begin{aligned}\tilde{F}(k_1,k_2) &= EE(k_1,k_2) + W_{3M}^{2k_2-k_1}EO(k_1,k_2) \\ &\quad + W_{3M}^{2k_1-k_2}OE(k_1,k_2) + W_{3M}^{k_1+k_2}OO(k_1,k_2) \\ \tilde{F}(k_1+\frac{3M}{2},k_2) &= EE(k_1,k_2) - W_{3M}^{2k_2-k_1}EO(k_1,k_2) \\ &\quad + W_{3M}^{2k_1-k_2}OE(k_1,k_2) - W_{3M}^{k_1+k_2}OO(k_1,k_2) \\ \tilde{F}(k_1+M,k_2+\frac{M}{2}) &= EE(k_1,k_2) + W_{3M}^{2k_2-k_1}EO(k_1,k_2) \\ &\quad - W_{3M}^{2k_1-k_2}OE(k_1,k_2) - W_{3M}^{k_1+k_2}OO(k_1,k_2) \\ \tilde{F}(k_1+5\frac{M}{2},k_2+\frac{M}{2}) &= EE(k_1,k_2) - W_{3M}^{2k_2-k_1}EO(k_1,k_2) \\ &\quad - W_{3M}^{2k_1-k_2}OE(k_1,k_2) + W_{3M}^{k_1+k_2}OO(k_1,k_2) \end{aligned} \tag{16}$$

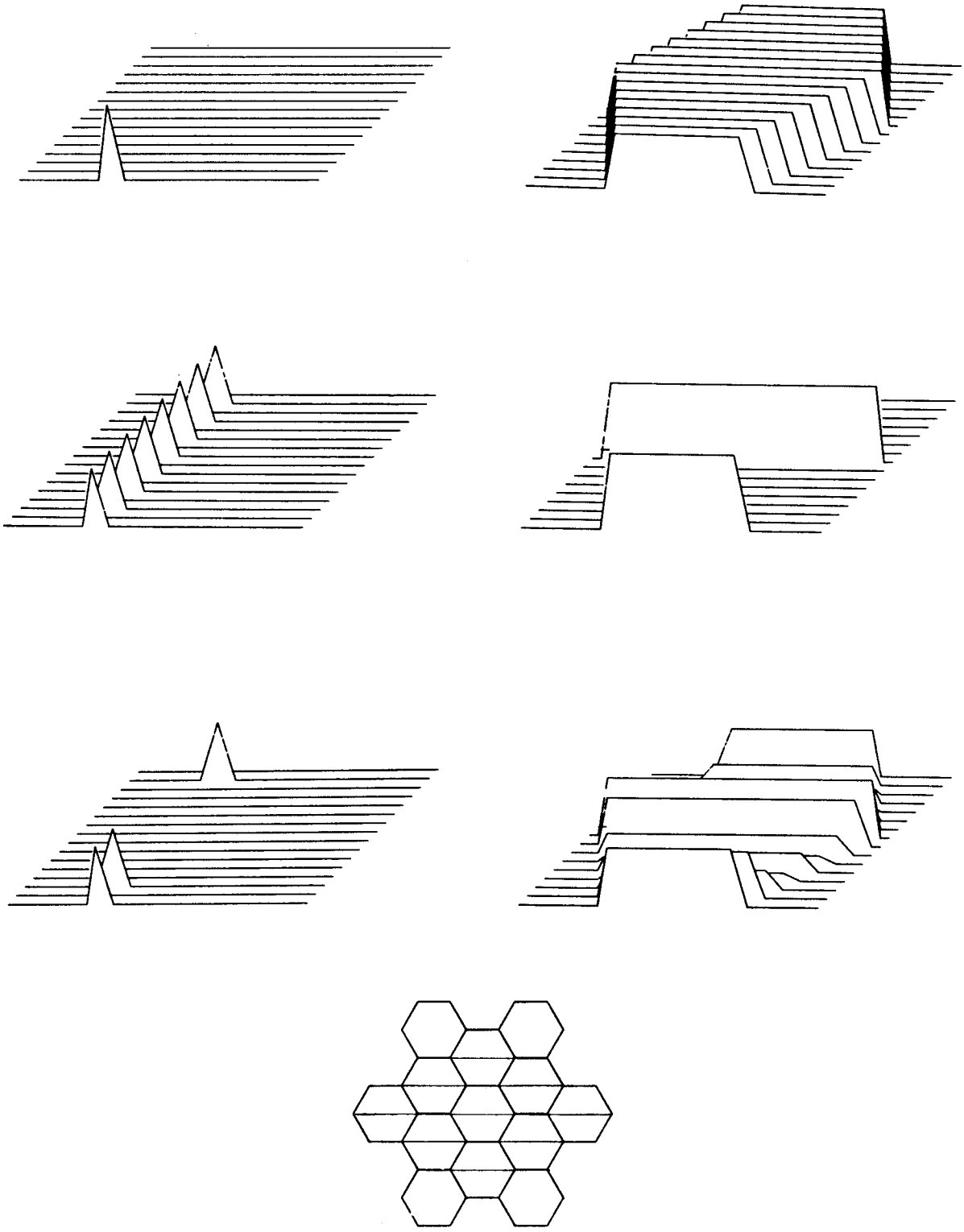

FIG. 5. DFT pairs for hexagonally sampled signals: hexagonal aliasing.

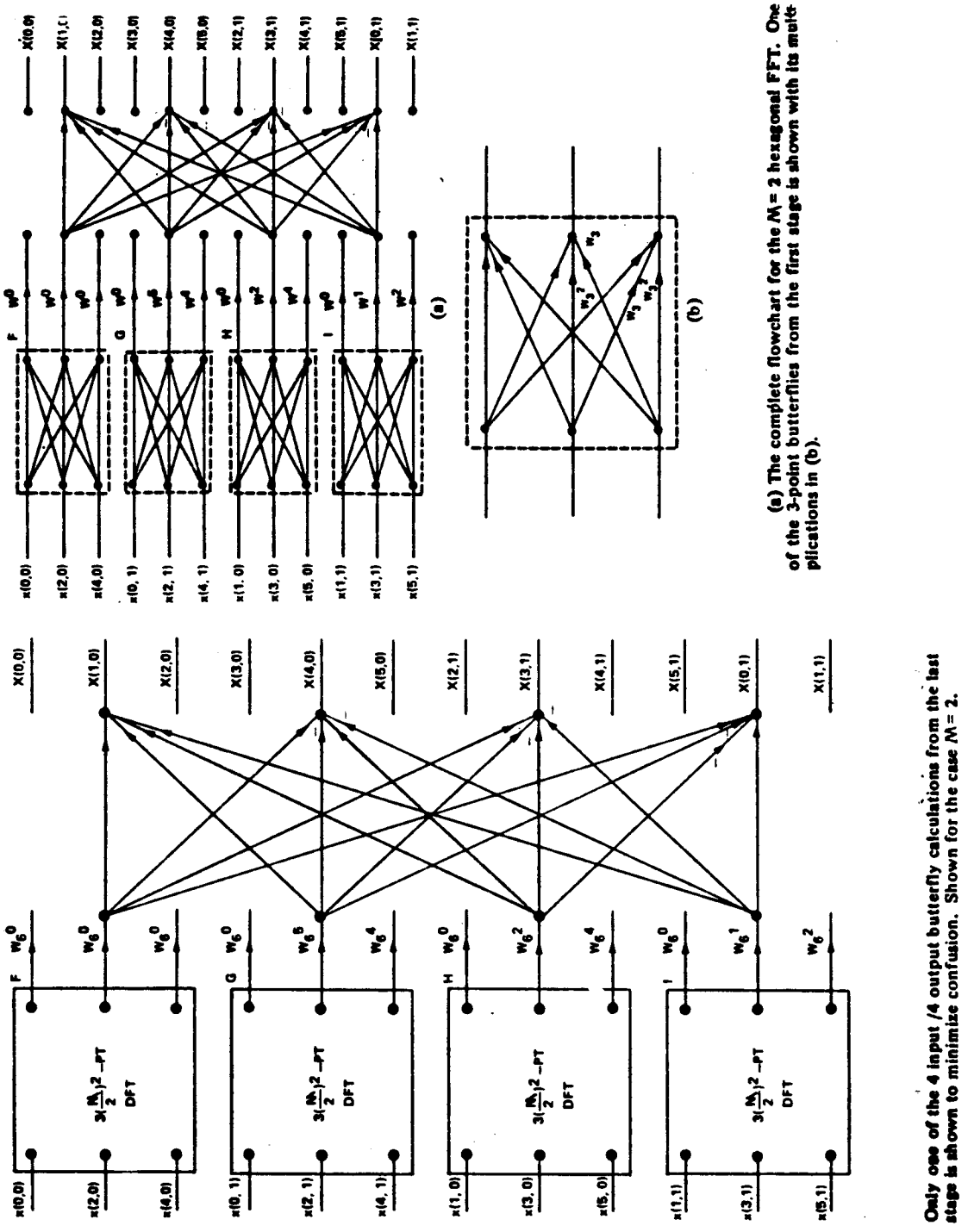


(a) The complete flowchart for the $M = 2$ hexagonal FFT. One of the 3-point butterflies from the first stage is shown with its multiplications in (b).

Only one of the 4 input /4 output butterfly calculations from the last stage is shown to minimize confusion. Shown for the case $M = 2$.

FIG. 6. FFT butterfly flowchart (Mersereau, 1979).

where $EE(k_1, k_2)$ represents the $DFT_{\frac{M}{2}}$ of the even/even $f(2r_1, 2r_2)$, etc. The algorithm's butterfly flowchart is shown in Figure 6 for M=2. The 25% savings in number of samples required for a given frequency resolution is preserved through application of the FFT—with $9M^2 log_2 M + 8M^2$ real multiplies required for the $3M^2$-point hexagonal DFT and $12M^2 log_2 M + 12M^2$ for the comparable $4M^2$-point rectangular DFT.

## Conclusion

The fundamental strength of a hexagonal sampling lattice is its great symmetry: a regular hexagon is 50% more symmetric than a square, exhibiting 12-fold as opposed to 8-fold symmetry. This symmetry forms the basis of all the efficiencies cited above, underlying the close approximation of a circular bandregion by a regular hexagonal bandregion. It also suggests that discrete hexagonal systems will be superior to rectangular systems wherever circularly symmetric functions are involved—a subject explored in the following paper by approximating a circularly symmetric filter with hexagonal difference stars. Finally, hexagonal sampling meshes permit a more symmetric view of any geophysical problem, if only by presenting a larger number of azimuths for profile studies and modelling.

## References

Mersereau, R.M., 1979, The processing of hexagonally sampled two-dimensional signals: Proc. IEEE, v. 67, p. 930-949.

Mersereau, R.M., and Speake, T.C., 1983, The processing of periodically sampled multidimensional signals: IEEE Trans. Acoust., Speech, Signal Processing, v. 31,p. 188-194.

Petersen, D.P., and Middleton, D., 1962, Sampling and reconstruction of wave-number-limited functions in N-dimensional Euclidean spaces: Information Control, v. 5, p. 279-323.

Gallagher, N.C., and Murphy, P.R., 1982, Hexagonal sampling techniques applied to Fourier and Fresnel digital holograms: J. Opt. Soc. Am., v. 72, no. 7, p. 929-937.